Desalination and Water Treatment
www.deswater.com

doi: 10.1080/19443994.2015.1129508

57 (2016) 22429–22440
October

Taylor & Francis
Taylor & Francis Group

Biosorption of Cd(II) and Cu(II) ions using *Lysinibacillus fusiformis* KMNTT-10: equilibrium and kinetic studies

K. Mathivanan, R. Rajaram*, V. Balasubramanian

Department of Marine Science, Bharathidasan University, Tiruchirappalli 620 024, Tamilnadu, India, email: kritamathi@gmail.com (K. Mathivanan), Tel. +91 431 2407111, ext. 418, +91 9842874661; Fax: +91 431 2407045; emails: drrajaram69@rediffmail.com (R. Rajaram), vbv82@rediffmail.com (V. Balasubramanian)

Received 8 April 2015; Accepted 2 December 2015

ABSTRACT

The biosorption of Cd(II) and Cu(II) ions from aqueous solutions on the biomass of *Lysinibacillus fusiformis* KMNTT-10 was investigated by batch method as functions of pH, contact time, biomass dose and initial metal concentrations. The experimental results showed the optimum pH for adsorption of Cd(II) and Cu(II) ions was 6.0, while the contact time was 2 h at room temperature (27 ± 2°C). The experimental data were successfully evaluated by isotherm and kinetic models. The maximum adsorption capacities (Q_{max}) for Cd(II) and Cu(II) ions obtained from the Langmuir equation were 53.19 and 46.29 mg g^{-1}, respectively. The adsorption kinetics for tested metals followed the pseudo-second-order model than the pseudo-first-order model. Scanning electron microscopic analysis showed deformation and surface damage in the Cd(II) and Cu(II) adsorbed cells. Energy-dispersive X-ray scanning results confirmed the adsorption of Cd(II) and Cu(II) onto biomass. Fourier transform-infrared spectroscopy analysis indicated that functional groups (amino, carboxyl, hydroxyl and carbonyl groups) on the cell surface were responsible for metal binding.

Keywords: Biosorption; Heavy metals; Isotherms; SEM–EDX analysis; Functional groups

1. Introduction

Heavy metal pollution in aquatic environment is caused by anthropogenic activities such as mining, electroplating, electric appliance manufacturing, discharging of metal containing municipal and industrial wastes and use of metal containing pesticides. Heavy metals are non-biodegradable persistent pollutant which causes serious environmental threat, and affecting human health via food chain. Especially, cadmium and copper are often used in many industries and released into the environment from a variety of industrial wastewaters. Over the past five decades, the worldwide release of cadmium and copper reached 22,000 and 939,000 t, respectively [1]. Particularly, cadmium and its compounds are highly toxic, mutagenic and carcinogenic [2,3], which damage the cells by binding with glutathione and sulphydryl groups in protein [4]. Copper, on the other hand, causes various health problems to living organisms; in particular, liver damage upon prolonged exposure [5]. Therefore, removal and recovery of heavy metals from wastewater is important for the protection of environment and human health. Conventional methods (precipitation, ion exchange, electroplating and/or membrane processes) of metal removal are expensive and inefficient

*Corresponding author.

at low concentrations (≤100 mg L^{-1}) [6,7]. Recently, the use of bio-based adsorbent has been considered as an alternative to remove the metals from wastewater. Compared with conventional methods, it can be an economical and efficient method at low concentrations [8,9]. Usually, it removes heavy metals without creating secondary pollution. Various biomasses such as microbes, plants and agricultural wastes were extensively used as adsorbents for removal of heavy metals. Amongst, microbial adsorbents (bacteria, algae, fungi, yeasts, etc.) appear to be more promising than other biosorbents. Of the other microbial adsorbents, bacterial biomass has received considerable attention because of (a) easier cultivation in laboratory, (b) rapid growth within the short period, (c) higher production yield under simple nutritional conditions and (d) high metal sorbing capacity because of higher surface area to volume ratio [10]. The cell wall of microbial adsorbent composed of polysaccharides, proteins and lipids, which containing many functional groups such as carboxylate, hydroxyl, sulphate, phosphate, amide and amino groups. These functional groups are actively involved in metal binding. Heavy metal biosorption depends on the chemical and physical properties of the metal ions, cellular physiology and cell viability as well as some external factors such as pH, temperature, biomass type and metal concentrations [11,12]. The strain *Lysinibacillus fusiformis* KMNTT-10 is a Gram-positive bacterium isolated from Uppanar estuarine water samples of Cuddalore coast, south-east coast of India, which has greater metal resistance and adsorbing abilities. The objective of the present study was to investigate the biosorption ability of *L. fusiformis* KMNTT-10 for Cd(II) and Cu(II) ions. The influences of solution pH, contact time, biomass dose and initial metal concentrations on the metal biosorption were studied by employing batch mode techniques. In addition to this, isotherm and kinetic models were used to evaluate the experimental data. The biosorbent nature and metal ions interaction was evaluated by scanning electron microscopy (SEM) coupled with energy-dispersive X-ray spectroscopy (EDX) and Fourier transform-infrared spectroscopy (FT-IR) analysis.

2. Materials and methods

2.1. Bacterial strain and biosorbent preparation

The bacterial strain *Lysinibacillus fusiformis* KMNTT-10 (GenBank Accession no. KC152467.1) used in this study was previously isolated from the polluted water samples of Uppanar estuary, south-east coast of India [13]. This strain has higher metal resistant (Cd(II), Cu(II), Pb(II) and Zn(II)) and biosorption capability under nutrient conditions. In order to prepare the biosorbent, the bacterial cells were cultured in 20% seawater nutrient broth (20% SWNA composition L^{-1}: 5.0 g peptone, 1.5 g beef extract, 1.5 g yeast extract, 200 mL aged seawater and 800 mL deionized water; salinity = 5 ± 2‰) for 24 h. Biomass was harvested by centrifugation at 8,000 rpm for 10 min. The collected biomass was washed thrice with distilled deionized water and used as an adsorbent for biosorption experiments.

2.2. Preparation of metals stock solutions

Analytical grade salts of $CdCl_2{\cdot}5H_2O$ (Loba Chemie, Mumbai, India) and $CuSO_4{\cdot}5H_2O$ (Fisher Scientific, Mumbai, India) were used to prepare the 1,000 mg L^{-1} of stock solutions. The stock solutions were sterilized at 110˚C for 15 min and filtered using 0.45-μm-pore size filters. The required concentrations of working solutions were obtained by appropriate dilution in deionized water prior to each experiment.

2.3. Biosorption experiments

The schematic representation of Cd(II) and Cu(II) biosorption by *L. fusiformis* KMNTT-10 biomass is illustrated in Fig. 1. Biosorption experiments were conducted by adding 0.1 g of biosorbent in 50 ml of 100 mg L^{-1} metal solution, and then mixtures were continuously stirred on a shaker (150 rpm) at room temperature (27 ± 2˚C). The mixtures were taken at desired intervals and were subsequently centrifuged at 5,000 rpm for 10 min at 4˚C. The metal concentrations in supernatants were estimated using the Atomic Absorption Spectrometer (GBC HG 3000; Sens AA, Australia; 2009). All experiments were carried out in triplicate for both metals. The effect of pH on the biosorption was investigated in the pH range 2–7. The initial pH of the working solutions were adjusted with of 0.1 N NaOH and 0.1 N HNO_3.

The effect of biomass dosage on biosorption was studied by adding different concentrations of biosorbent (0.05–0.2 g) in 50 ml of 100 mg L^{-1} metal solution.

The effect of contact time on biosorption was carried out in 100-mL flask containing 100 mg L^{-1} of Cd (II) and Cu(II) solution (50 mL) and 0.1 g of biosorbent. Samples were taken at different time intervals (0–4 h) and analyzed as described above.

For adsorption isotherms, 0.1 g of biosorbent was added in 50 mL of different concentrations (50–300 mg L^{-1}) of Cd(II) and Cu(II) solution at optimized pH value of 6.0. The mixtures were continuously stirred on a shaker (150 rpm) at room temperature (27

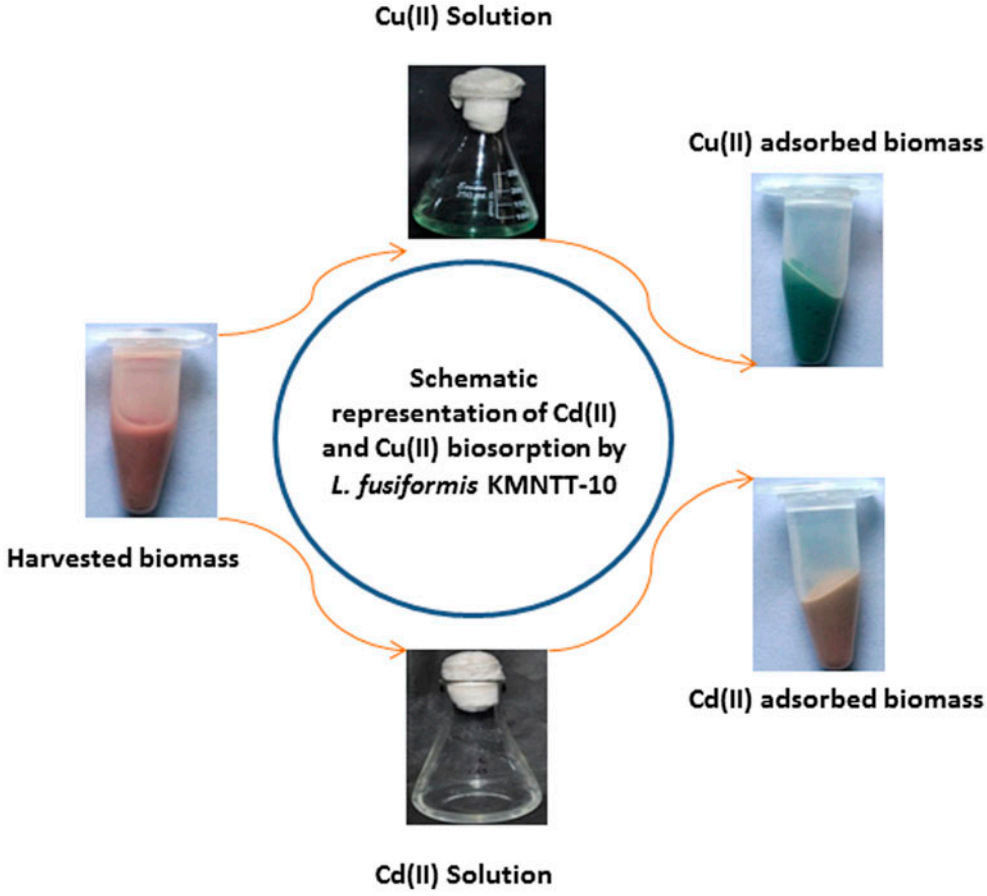

Fig. 1. Schematic representation of Cd(II) and Cu(II) biosorption by harvested biomass of *L. fusiformis* KMNTT-10.

± 2°C) for 2 h. After 2 h, the mixtures were taken and then followed the same procedure as described above. The biosorption capacity (q_e) can be calculated as follows:

$$q_e\ (\mathrm{mg\,g^{-1}}) = \frac{[C_i - C_e]}{M} \times V \quad (1)$$

where C_i and C_e are the initial and equilibrium concentrations of metal (mg L^{-1}), respectively. M = weight of biosorbent (g), V = solution volume (L).

2.4. Scanning electron microscopy (SEM) and energy-dispersive X-ray analysis (EDX)

The metal-adsorbed and non-adsorbed cells were obtained by centrifugation (10,000 rpm at 4°C for 10 min) and washed thoroughly with sodium phosphate buffer (0.1 M, pH 7.2), fixed overnight in 2.5% glutaraldehyde (prepared in 0.1 M PBS). The cells were smeared on the glass slides and dehydrated in a series of increasing concentrations (10% to absolute) of ethanol. The air-dried slides were firmly fixed on brass stub, sputter-coated with gold and viewed by SEM (JSM-5610LV, JEOL, JAPAN). EDX (OXFORD ISIS 300 EDS) was used to confirm the adsorption of Cd(II) and Cu(II) by biosorbent.

2.5. FTIR analysis of biosorbent

The metal (Cd(II) and Cu(II))-adsorbed and non-adsorbed cells were dried in an oven at 60°C. The dried cells were powdered and mixed with KBr to make a disc for spectrum analysis. The disc was scanned using an FT-IR spectrophotometer (Spectrum RX I, Perkin Elmer, USA) in the range of 4,000–400 cm^{-1}.

3. Results and discussion

3.1. Effect of pH on biosorption

The solution pH is the most important parameter which affects the sorption capacity of biosorbent [14]. The effect of pH on Cd(II) and Cu(II) biosorption is

presented in Fig. 2. Results showed that the biosorption capacity of biomass for both metals increased with an increase in pH until reaching the optimum at 6.0, and then decreased at pH value above 6.0. The maximum biosorption capacity for Cd(II) and Cu(II) observed at pH 6.0 was 41.6 and 38.7 mg g^{-1}, respectively. Metal biosorption is achieved through ionic interaction between metals and functional groups (carboxyl, phosphate, imidazole and amino groups) of the biomass. It is reported that at lower pH, the hydrogen (H^+) and hydronium (H_3O^+) ions are greater in solution which competes with cations for binding sites of cells. In addition, the hydrogen (H^+) and hydronium (H_3O^+) ions protonate the cell surface of biomass which limits the binding of metals with cells. At increased pH, the biosorption capacity increased due to the decreased competing effect of these protons (H^+ and H_3O^+) with cations [15]. It is previously reported that the solution pH affects the net negative charge on the cell surface as well as the availability of metal ions [10]. However, at pH values above 6.0, the metal ions precipitate as metal hydroxides because of the high concentrations of OH^- ions in the solution [16]. Reddy et al. [17] reported that decreased adsorption at pH > 6 was due to the formation of soluble hydroxylated metal complexes and their competition with the binding sites. The solution pH affects not only the surface charge of the biosorbent but also the metal speciation. Metal speciation is a vital process in the metal adsorption which is pH dependent. The metal can exist in various forms in solution as a function of pH. It is reported that copper exists as Cu^{2+} at pH 3.0–4.0; $Cu(OH)^+$ at pH 4.0–5.0 and $Cu(OH_2)$ at pH > 6 [18]. For cadmium, Cd^{2+} ions are predominant at pH values between 3.5 and 5.0, whereas low-soluble species such as $Cd(OH)_2$ and $Cd(OH)_3$ at pH > 5.0 [19]. Moreover, the metal speciation process in adsorption solution depends not only on pH but also on adsorbate–adsorbent concentrations.

3.2. Effect of biomass dosage on biosorption

The effect of biomass dosage on Cd(II) and Cu(II) biosorption is shown in Fig. 3. The results showed that biosorption capacity decreased by increasing the biomass dosage for both metal ions. As shown in Fig. 3, when the biomass dosage was increased from 0.05 to 0.2 g, the biosorption capacity decreased from 79.4 to 16.0 mg g^{-1} for Cd(II) and from 73.8 to 15.3 mg g^{-1} for Cu(II). The results confirmed that the biomass dosage strongly affected the biosorption capacity. The highest biosorption capacity for both metals was observed at low biomass dosage, and this might be due to the availability of free adsorption sites. The decreased biosorption capacity was observed at higher biomass dosage for both metals. This may be due to electrostatic interaction between cells, which decrease the binding sites for metal occupation [20,21].

3.3. Effect of contact time on biosorption

Contact time is another important parameter which influences the biosorption process. Fig. 4 shows the effect of contact time for the biosorption of Cd(II) and Cu(II) onto KMNTT-10 biosorbent. Results indicate that biosorption capacity for Cd(II) and Cu(II) ions was rapid and attained equilibrium within 2 h of contact time. The maximum biosorption of 42.5 mg g^{-1} for Cd(II) and 37.1 mg g^{-1} for Cu(II) was observed at 2 h of contact time. The biosorption occurred in two phases: an initial phase of faster adsorption and later

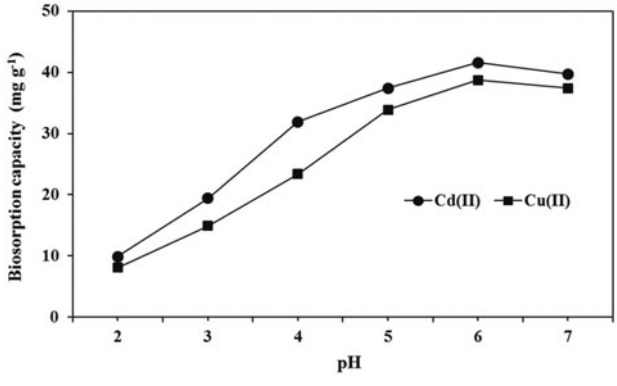

Fig. 2. Effect of pH on Cd(II) and Cu(II) biosorption (experimental conditions: initial concentration 100 mg L^{-1}; biosorbent dose 0.1 g; contact time 12 h).

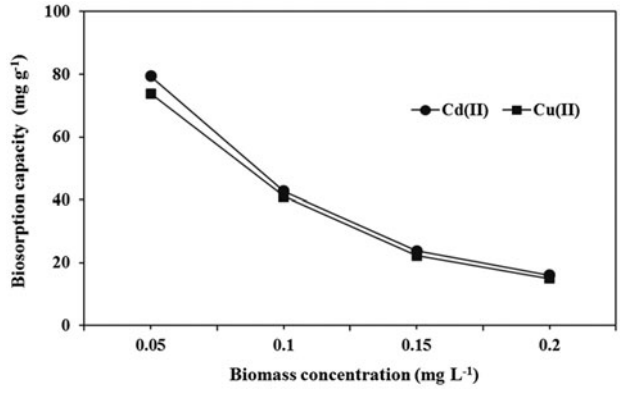

Fig. 3. Effect of biomass concentration on Cd(II) and Cu(II) biosorption (experimental conditions: initial concentration 100 mg L^{-1}; pH 6.0; contact time 12 h).

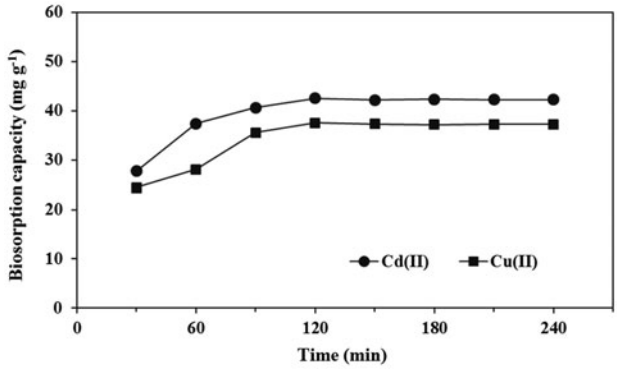

Fig. 4. Effect of contact time on Cd(II) and Cu(II) biosorption (experimental conditions: initial concentration 100 mg L^{-1}; pH 6.0; biosorbent dose 0.1 g).

phase of lower adsorption [22]. The initial phase takes shorter time to metal sorption, and this might be due to availability of abundant metal species and empty metal binding sites of the biomass. Lower metal uptake at the later stage may be due to saturation of binding sites and/or intra-particle diffusion process [23]. Ziagova et al. [14] reported similar behaviour for the biosorption of Cd(II) and Cr(VI) on *Staphylococcus xylosus* and *Pseudomonas* sp. in single and binary mixtures.

3.4. Effect of initial metal concentration on biosorption

Fig. 5 shows the effect of initial metal concentration for the biosorption of Cd(II) and Cu(II) ions. The results showed that the sorption capacity of biomass increased by increasing the initial concentration of metal ions. For Cd(II), when the initial metal concentration was increased from 50 to 300 mg L^{-1}, the sorption capacity increased from 23.2 to 54.5 mg g^{-1}. In case of Cu(II), the sorption capacity increased from 21.4 to 47.4 mg g^{-1} (Fig. 5). The experimental result indicating biosorption process depends not only on the properties of biomass, but also on the metal ions concentration in solution. The increased biosorption rate at higher concentration might be due to diffusion of metal ions into the biomass by intra-particular diffusion and/or binding of metal ions with released biomaterials through cell damage. The Cd(II) biosorption capacity was found to be considerably higher vs. Cd (II), and this might be attributed to the difference in their ionic radii [24]. The ionic radii of Cd(II) and Cu (II) are 0.97 and 0.73 Å, respectively. In general, the smaller the ionic radius, the greater its tendency to be hydrolyzed, leading to reduced adsorption. So, Cu(II) has a greater tendency to be hydrolyzed than Cd(II). For this reason, the biosorbent has greater affinity for Cd(II) than Cu(II). Similar result was reported previously for metal biosorption under the influences of initial metal concentration using *Phanerochaete chrysosporium* biomass [25], lyophilized *Pseudomonas stutzeri* [26] and *Geobacillus thermantarcticus* [27].

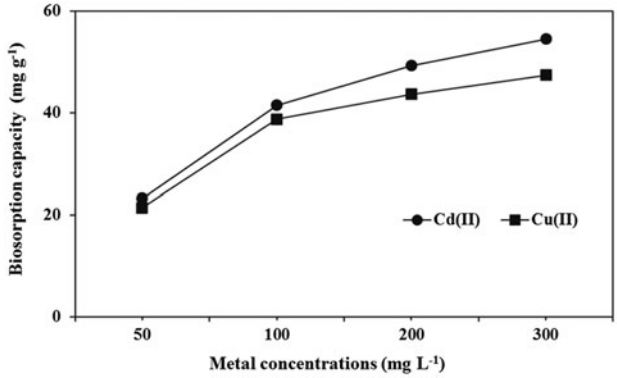

Fig. 5. Effect of initial metal ion concentration on Cd(II) and Cu(II) biosorption (experimental conditions: biosorbent dose 0.1 g; pH 6.0; contact time 2 h).

3.5. Adsorption isotherms

The biosorption capacity of an adsorbent can be described by its equilibrium sorption isotherm, which is characterized by certain constants which express the surface properties and affinity of the adsorbent [28]. To test the fit of data, the Langmuir and Freundlich isotherm models were applied in this study. The linearized Langmuir and Freundlich isotherms were used to describe the equilibrium state for single-ion biosorption.

The Langmuir isotherm assumes a monolayer adsorption of solute onto a solid surface with a finite number of identical sites. The mathematical description of the Langmuir equation is:

$$q_e = \frac{Q_{max} b C_e}{1 + b C_e} \tag{2}$$

By plotting the linear form of Eq. (2):

$$\frac{C_e}{q_e} = \frac{1}{Q_{max} b} + \frac{C_e}{Q_{max}} \tag{3}$$

where Q_{max} (mg g^{-1}) is the maximal metal sorption capacity, b (l mg^{-1}) represents the sorption equilibrium constant. Q_{max} and b can be determined experimentally by plotting of C_e/q_e vs. C_e (Fig. 6(a)). The value

of Langmuir constant b (l mg^{-1}) represents biomass–metal binding affinity [29].

The Freundlich isotherm is an empirical equation based on sorption on a heterogeneous surface. This empirical equation of the Freundlich isotherm is:

$$q_e = K_F C_e 1/n \quad (4)$$

By plotting the linear form of Eq. (4):

$$\log q_e = \frac{1}{n} \log C_e + \log K_F \quad (5)$$

where K_F and n are Freundlich adsorption capacity constant and adsorption intensity, respectively. The value of K_F and n was determined by plotting log q_e vs. log C_e (Fig. 6(b)). The linearized Langmuir and Freundlich adsorption isotherms of *L. fusiformis* biomass for Cd(II) and Cu(II) were shown in Fig. 6(a) and (b). The Langmuir and Freundlich adsorption constants and its corresponding correlation coefficients were given in Table 1. The maximum adsorption capacity (Q_{max}) of biomass for Cd(II) and Cu(II) obtained from Langmuir equations was 53.19 and 46.29 mg g^{-1}, respectively (Table 1). Experimental Cd(II) and Cu(II) adsorption data were correlated and had similarity with the Langmuir model with R^2 value of 0.993 and 0.992, respectively. The Q_{max} values indicated that Cd (II) ions were greatly adsorbed by biomass from aqueous solution compared to Cu(II) ions. The Langmuir results showed that tested biomass has the greater adsorptive capacity and could be used for biosorption of Cd(II) and Cu(II) from polluted wastewaters. The adsorption capacity of *L. fusiformis* KMNTT-10 biosorbent for both metals appears to be higher in comparison with those other biosorbent (Table 2). The experimental adsorption data were also correlated with the Freundlich model. The adsorption capacity constants (K_F) and adsorption intensity (n) for Cd(II) obtained from Freundlich isotherm were 19.78 and 4.95, respectively. In case of Cu(II), the adsorption capacity constants (K_F) and adsorption intensity (n) were 16.91 and 4.75, respectively. When approaching the adsorption intensity value (n) to 1 or greater than 1, indicates that the adsorbate was effectively adsorbed by biosorbent [32]. Results showed that intensity value (n) of biosorbent for both metals was greater than 1, which indicates that Cd(II) and Cu(II) ions effectively adsorbed under studied condition. The magnitude of K_F and n clearly showed that the isolate was adsorbed Cd(II) from aqueous solution with a high adsorptive capacity compared to Cu(II). As shown in Table 1, the regression coefficient (R^2) values from Langmuir isotherm were greater than those of Freundlich isotherm. All these results showed the Langmuir isotherm model fitted the adsorption data quite well than the Freundlich isotherm.

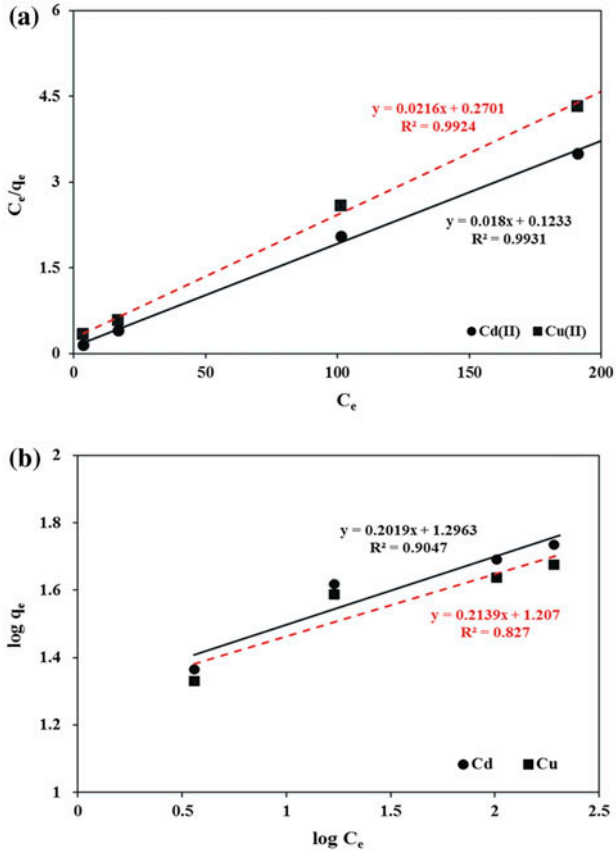

Fig. 6. The linear form of Langmuir adsorption (a) and Freundlich adsorption (b) isotherm for Cd(II) and Cu(II).

3.6. Adsorption kinetics

The kinetic models such as pseudo-first-order and pseudo-second-order were used to describe the adsorption kinetics. The rate constants of Cd(II) and Cu(II) adsorption by *L. fusiformis* KMNTT-10 biomass

Table 1
Isotherm model constants for absorption of Cd(II) and Cu (II) on bacterial biomass

	Langmuir			Freundlich		
Metals	Q_{max}	b	R^2	K_F	n	R^2
Cd(II)	53.19	0.083	0.993	19.78	4.953	0.905
Cu(II)	46.29	0.069	0.992	16.10	4.675	0.827

Table 2
Comparison of biosorption capacity of *L. fusiformis* KMNTT-10 for Cd(II) and Cu(II) with those other biosorbents

Metal	S. no.	Biosorbent	Sorption capacity (mg g^{-1})	Refs.
Cd(II)	1	*Geobacillus thermantarcticus*	33.78	[27]
	2	*P. simplicissimum*	52.5	[30]
	3	*Pseudomonas stutzeri*	47.86	[26]
	4	*L. fusiformis* KMNTT-10	53.19	Present study
	5	*Anoxybacillus amylolyticus*	18.72	[27]
Cu(II)	1	*Pantoea* sp. TEM18	31.3	[31]
	2	*A. amylolyticus*	12.39	[27]
	3	*Pseudomonas stutzeri*	33.16	[26]
	4	*L. fusiformis* KMNTT-10	46.29	Present study
	5	*Geobacillus thermantarcticus*	24.21	[27]

were determined using the pseudo-first-order kinetic model. The linear form of pseudo-first-order model is given below [33]:

$$\log(q_e - q_t) = \log q_e - \frac{k_1}{2.303}t \quad (6)$$

where q_e and q_t are the amount of metal adsorption at equilibrium state and at any time, respectively (mg g^{-1}). k_1 (min^{-1}) is the pseudo-first-order rate constant. The value of k_1 was obtained experimentally by plotting $\log(q_e - q_t)$ vs. t (Fig. 7).

The linear form of pseudo-second-order model is expressed as follows [34]:

$$\frac{t}{q_t} = \frac{1}{k_2 q_e^2} + \frac{1}{q_t}t \quad (7)$$

where k_2 is the rate constant of the pseudo-second-order kinetic model (g mg^{-1} min^{-1}). The q_e and k_2 were obtained by extrapolation of the linear portion of the plot of t/q_t vs. t (Fig. 8). The pseudo-first-order and pseudo-second-order kinetic models are shown in Figs 7 and 8. The rate constants and correlation coefficient values for both metals were depicted in Table 3. As shown in Table 3, the calculated q_e value for both metals from the pseudo-first-order model is not closer to experimental q_e value. Compared with the pseudo-first-order model, the pseudo-second-order model was fitted well with the experimental data with high correlation coefficient [35]. The q_e value of 42.84 mg g^{-1} (Cd(II)) and 36.36 mg g^{-1} Cu(II)) calculated from pseudo-second-order model fitted well with experimental data of 42.5 and 37.5 mg g^{-1}, respectively. Therefore, pseudo-second-order kinetic model is suitable to describe the adsorption kinetics of Cd(II) and Cu(II) by KMNTT-10.

3.7. Scanning electron microscopy and energy-dispersive X-ray analysis

The morphology of metal adsorbed and non-adsorbed biomass is shown in Fig. 9(a)–(c). The mor-

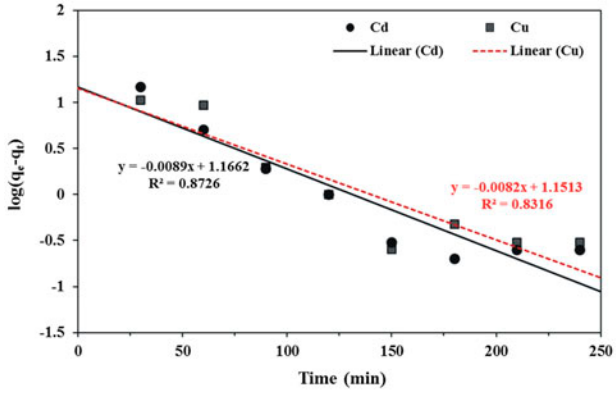

Fig. 7. Pseudo-first-order kinetics of Cd(II) and Cu(II) adsorption for KMNTT-10 biomass.

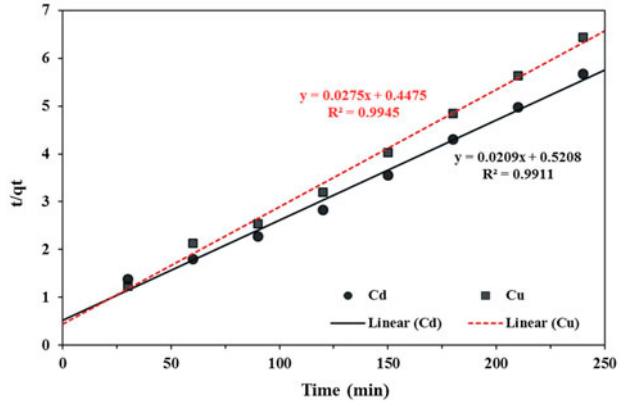

Fig. 8. Pseudo-second-order kinetics of Cd(II) and Cu(II) adsorption for KMNTT-10 biomass.

Table 3
Kinetic parameters for the biosorption of Cd(II) or Cu(II) onto *L. fusiformis* KMNTT-10

	Pseudo-first-order			Pseudo-second-order			
Metal	k_1 (min^{-1})	R^2	$q_{e(cal)}$ (mg g^{-1})	k_2 (g mg^{-1} min^{-1})	R^2	$q_{e(cal)}$ (mg g^{-1})	$q_{e(exp)}$ (mg g^{-1})
Cd(II)	0.020	0.872	14.7	0.0008	0.991	42.84	42.5
Cu(II)	0.018	0.831	14.2	0.0615	0.994	36.36	37.5

phology of bacterial cells was typical rod shape and smooth surface. However, the morphology of cells after Cd(II) and Cu(II) adsorption was drastically changed. SEM image of Fig. 9(b) and (c) clearly displayed the appearance of irregular bulge (blebs) on its outer membrane of Cd(II)- and Cu(II)-adsorbed cells. In fact, the changes in the surface morphology of metal-adsorbed cells are an adopted mechanism to resist the heavy metal toxicity [36]. Highem et al. [37] stated the size of the cadmium-treated *Pseudomonas putida* cells was smaller than non-treated cells, and formed blister-like protrusions (blebs) in the surface structure of cadmium-treated cells. Adarsh et al. [38] reported that distinct changes in cell size and surface features of metal-adsorbed bacterial cells as compared to non-adsorbed cells. The EDX spectra of metal-adsorbed cells clearly showed the presence of peaks pertaining to cadmium and copper, which were not appeared in EDX spectrum of non-adsorbed cells. These results confirmed the adsorption of Cd(II) and Cu(II) on the KMNTT-10 biomass.

3.8. FTIR analysis of biosorbent

FTIR spectra of the control (metal non-adsorbed) and metal-adsorbed biomass were recorded to study the functional groups involved in metal binding (Fig. 10(a)–(c)). Analyzing the IR spectra, the changes in peaks position and intensities were observed in metal-adsorbed biomass from its native position (control). The broad and strong peak at 3,300 cm^{-1} indicated the overlapping of –OH and –NH stretching vibration. The absorption peak at 2,929 cm^{-1} in the spectrum of control biomass could be attributed to the –CH stretching vibrations of $-CH_3$ and $=CH_2$ groups. A sharp and medium peak at 2,358 cm^{-1} exhibited to the asymmetric stretching of the isocyanate group (–N=C=O) [39]. While the absorption peaks at 1,653 and 1,539 cm^{-1} could be attributed to the amide I and amide II bands, respectively. The amide I and amide II in the spectrum could be attributed to the occurrence of protein in the biomass [40]. The peaks at 1,455 and 1,395 cm^{-1} might be attributed to C=O symmetric stretching of carboxyl salts (–COOH). Further, the peak at 1,233 cm^{-1} can be assigned to the vibrations of carboxyl (–COOH) and phosphate groups (P=O and P–O of the C–PO_3^{2-} moiety). Mostly, these groups belong to cellular components like phospholipids, peptidoglycan, cell-associated polysaccharides and peptides which are able to bind with metals [41]. The strong peak at 1,066 cm^{-1} was attributed to C–O stretching of alcohols and carboxylic acids [42]. The peak in the finger print region, i.e. 667 and 552 cm^{-1}, attributed with –C–C stretching. Overall, the IR spectra indicated that main functional groups presented on the biomass surface were hydroxyl, carbonyl, carboxyl, amide, imidazole, phosphate and phosphodiester groups. However, the significant changes in certain peak position and intensities were observed after metal adsorption (Fig. 10(b) and (c)). The spectra of Cd(II)- and Cu(II)-adsorbed biomass showed a minor shift in the peak position of 3,300 to 3,302 cm^{-1} and to 3,301 cm^{-1}, respectively. The significant change in the peak position and intensity at 2,358 cm^{-1} region after Cd(II) and Cu(II) biosorption were 2,359 and 2,362 cm^{-1}, respectively. These significant change in peak position and intensity after metal adsorption revealed that isocyanate groups are principally involved in the metal adsorption. Moreover, these significant changes may shift the other functional groups slightly from its native position [43]. The peaks wavelength observed at 1,653 and 1,539 cm^{-1} changed to 1,655 and 1,537 cm^{-1} for Cd(II) and to 1,656 and 1,538 cm^{-1} for Cu(II) adsorbed spectra, respectively. This might be due to these peaks corresponding functional groups amide I and amide II participated in metal binding. The peak at 1,455 cm^{-1} was shifted to 1,454 cm^{-1} in the metal-adsorbed biomass, which indicated the role of carboxyl groups in metal adsorption. Compared with native spectrum, the peaks at 2,929 and 1,233 cm^{-1} were not shifted in the spectrum of Cd (II)-treated biomass (Fig. 10(b)). In the spectrum of Cu (II)-adsorbed biomass, the peak at wavelength of 1,395 cm^{-1} was not shifted from its native position (Fig. 10(c)). The non-shifted peaks corresponding functional groups did not participate in the metal biosorption [35]. The significant changes in certain peaks position after metal adsorption indicate that peaks

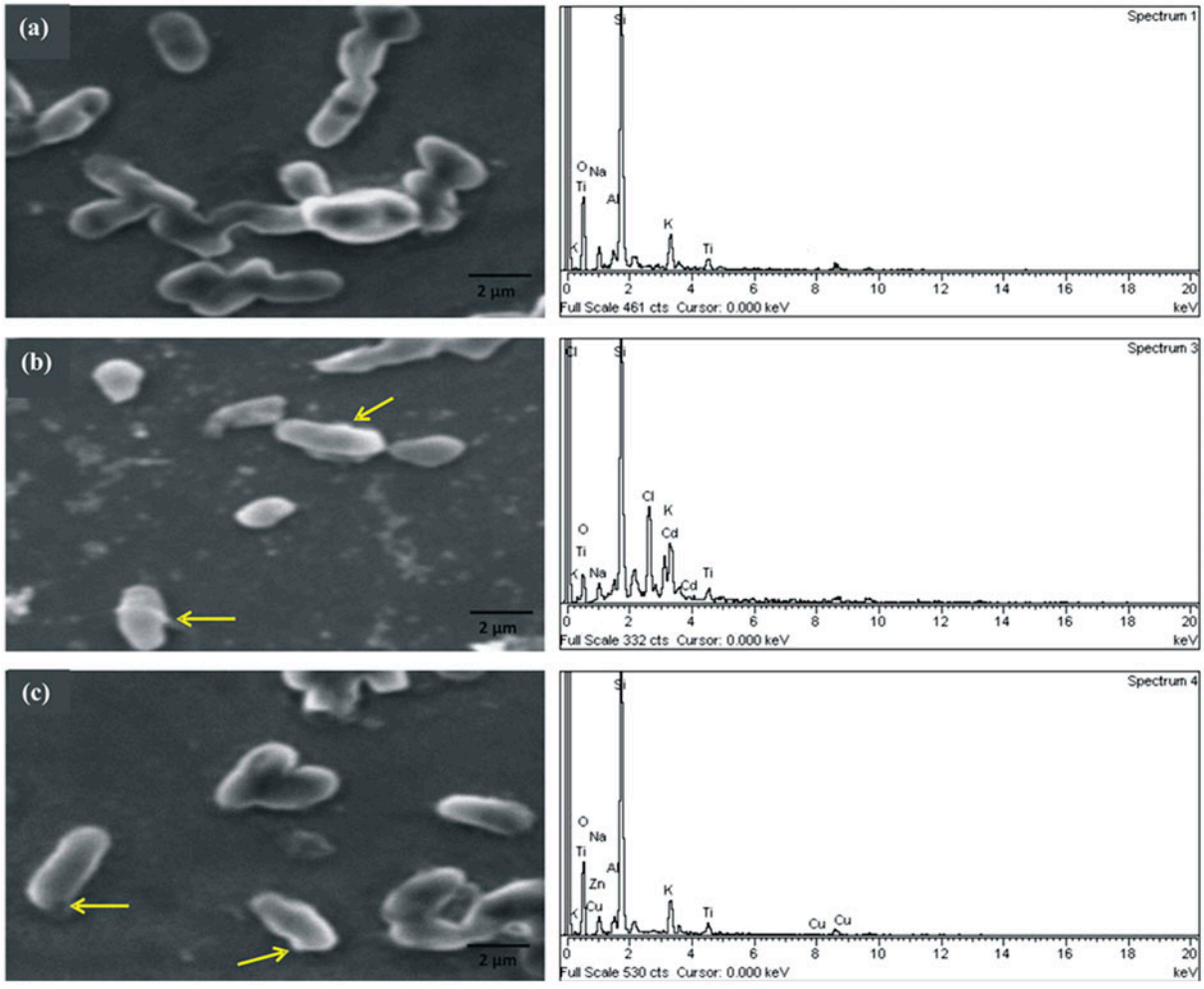

Fig. 9. SEM–EDX analysis of *L. fusiformis* KMNTT-10 after and before Cd(II) and Cu(II) biosorption: (a) Metal non-adsorbed cells; (b) Cd(II)-adsorbed cells and (c) Cu(II)-adsorbed cells (arrow indicates "blebs").

corresponding functional groups involved in the metal binding [36,42].

3.9. Adsorption mechanism discussion

Understanding the mechanisms of metal–bacterial interaction is important for the selection of suitable strain to develop the effective and economically feasible biosorption process [44]. In the present study, the adsorption mechanisms of bacteria with metals were investigated by SEM–EDS and FTIR analysis. The cells before metal adsorption were typically rod shaped and have smooth surface (Fig. 9(a)). However, the morphology of cells after metal adsorption was drastically changed and displayed the irregular bulge on the cell wall (Fig. 9(b) and (c)). The changes in cell wall of bacteria are a defence process against metal toxicity [36]. Moreover, the results suggested that cell wall of bacteria is the primary site for metal binding. The EDX spectra confirmed the adsorption of Cd(II) and Cu(II) on the KMNTT-10 biomass. Generally, metal biosorption is accomplished through interaction of metals with functional groups of cell wall. FTIR spectra showed various functional groups present on the cell wall such as hydroxyl, carbonyl, carboxyl, amide, imidazole, phosphate and phosphodiester groups. These functional groups are mainly present in the cell wall constituents such as polysaccharides, proteins and lipids. When analyzing the IR spectra, significant changes were observed at peaks wavelength and also the intensity in the spectra of biomass after metal adsorption (Fig. 10(b) and (c)). These spectral changes provide evidence for the functional groups of cell surface as a primary site for metal adsorption [37]. In addition, the solution pH can affect the negative charge of functional groups during metal biosorption.

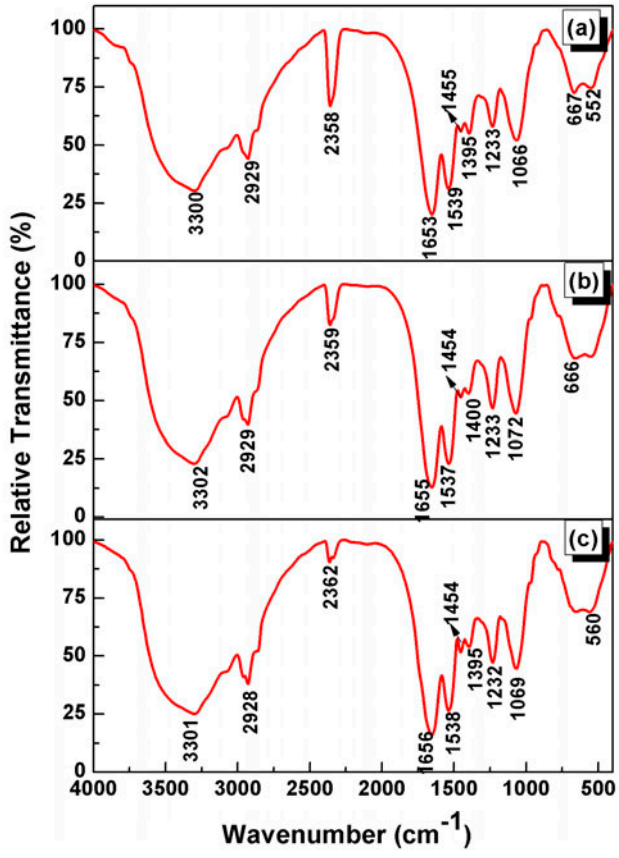

Fig. 10. Fourier transformed IR spectra of *L. fusiformis* KMNTT-10 biomass: (a) non-adsorbed cells, (b) Cd(II)-adsorbed cells and (c) Cu(II)-adsorbed cells.

The results obtained from the effect of pH on metal adsorption indicate that ion exchange between functional groups with metals is controlled by solution pH [10,15]. Overall, the study results showed the metal adsorption onto biomass is a combined process of ion-exchange–complexation.

4. Conclusions

In this study, the biomass of *L. fusiformis* KMNTT-10 efficiently removed the Cd(II) and Cu(II) from aqueous solutions. The physicochemical conditions such as pH, contact time, initial concentration of metal and biomass strongly affected the biosorption processes. The optimum conditions for Cd(II) and Cu(II) adsorption were pH 6.0 and contact time 2 h at room temperature (27 ± 2°C). The maximum Cd(II) and Cu (II) biosorption capacities (Q_{max}) of biomass obtained from the Langmuir isotherm was 53.63 and 46.27 mg g^{-1}, respectively. The kinetic data of Cd(II) and Cu(II) biosorption fitted well to the pseudo-second-order model than the pseudo-first-order model. SEM–EDX results confirmed that the biosorption of Cd(II) and Cu(II) by the biomass of *L. fusiformis* KMNTT-10. The FT-IR results revealed that the functional groups on the cell surface were principally involved in metal sorption. Overall, the study results showed that *L. fusiformis* KMNTT-10 biomass could be an effective adsorbent for the removal of heavy metals from wastewater.

Acknowledgements

Authors are thankful to the authorities of Bharathidasan University for the infrastructure facilities and acknowledge the University Grant Commission (UGC), Government of India for providing the financial support in carrying out this work (reference no. F. No. 36-55/2008 (SR) dated: 24-03-2009).

References

[1] O.V. Singh, S. Labana, G. Pandey, R. Budhiraja, R.K. Jain, Phytoremediation: An overview of metallic ion decontamination from soil, Appl. Microbiol. Biotechnol. 61 (2003) 405–412.
[2] M.P. Waalkes, M.R. Anver, B.A. Diwan, Chronic toxic and carcinogenic effects of oral cadmium in the Noble (NBL/Cr) rat: Induction of neoplastic and proliferative lesions of the adrenal, kidney, prostate, and testes, J. Toxicol. Environ. Health Part A 58 (1999) 199–214.
[3] S. Satarug, M.R. Moore, Adverse health effects of chronic exposure to low-level cadmium in foodstuffs and cigarette smoke, Environ. Health Perspect. 112 (2004) 1099–1103.
[4] P. Banjerdkij, P. Vattanaviboon, S. Mongkolsuk, Exposure to cadmium elevates expression of genes in the OxyR and OhrR regulons and induces cross-resistance to peroxide killing treatment in *Xanthomonas campestris*, Appl. Environ. Microbiol. 71 (2005) 1843–1849.
[5] A. Sánchez, A. Ballester, M.L. Blázquez, F. González, J. Muñoz, A. Hammaini, Biosorption of copper and zinc by *Cymodocea nodosa*, FEMS Microbiol. Rev. 23 (1999) 527–536.
[6] S.S. Ahluwalia, D. Goyal, Microbial and plant derived biomass for removal of heavy metals from wastewater, Bioresour. Technol. 98 (2007) 2243–2257.
[7] A.A.S. Al-Gheethi, I. Norli, J. Lalung, A. Megat Azlan, Z.A. Nur Farehah, M.O. Ab. Kadir, Biosorption of heavy metals and cephalexin from secondary effluents by tolerant bacteria, Clean Technol. Environ. Policy 16 (2014) 137–148.
[8] P. Sannasi, J. Kader, B.S. Ismail, S. Salmijah, Sorption of Cr(VI), Cu(II) and Pb(II) by growing and non-growing cells of a bacterial consortium, Bioresour. Technol. 97 (2006) 740–747.
[9] K. Mathivanan, R. Rajaram, Tolerance and biosorption of cadmium(II) ions by highly cadmium resistant bacteria isolated from industrially polluted estuarine environment, Indian J. Geo-Mar. Sci. 43 (2014) 580–588.

[10] A.I. Zouboulis, M.X. Loukidou, K.A. Matis, Biosorption of toxic metals from aqueous solutions by bacteria strains isolated from metal-polluted soils, Process Biochem. 39 (2004) 909–916.
[11] R.F. Unz, K.L. Shuttleworth, Microbial mobilization and immobilization of heavy metals, Curr. Opin. Biotechnol. 7 (1996) 307–310.
[12] F. Veglio, F. Beolchini, Removal of metals by biosorption: A review, Hydrometallurgy 44 (1997) 301–316.
[13] K. Mathivanan, R. Rajaram, Isolation and characterisation of cadmium-resistant bacteria from an industrially polluted coastal ecosystem on the southeast coast of India, Chem. Ecol. 30 (2014) 622–635.
[14] M. Ziagova, G. Dimitriadis, D. Aslanidou, X. Papaioannou, E. Litopoulou-Tzannetaki, M. Liakopoulou-Kyriakides, Comparative study of Cd(II) and Cr (VI) biosorption on *Staphylococcus xylosus* and *Pseudomonas* sp. in single and binary mixtures, Bioresour. Technol. 98 (2007) 2859–2865.
[15] A. Suazo-Madrid, L. Morales-Barrera, E. Aranda-García, E. Cristiani-Urbina, Nickel(II) biosorption by *Rhodotorula glutinis*, J. Ind. Microbiol. Biotechnol. 38 (2001) 51–64.
[16] T. Halttunen, S. Salminen, R. Tahvonen, Rapid removal of lead and cadmium from water by specific lactic acid bacteria, Int. J. Food Microbiol. 114 (2007) 30–35.
[17] D.H.K. Reddy, D.K.V. Ramana, K. Seshaiah, A.V.R. Reddy, Biosorption of Ni(II) from aqueous phase by *Moringa oleifera* bark, a low cost biosorbent, Desalination 268 (2011) 150–157.
[18] R.A.K. Rao, S. Ikram, Sorption studies of Cu(II) on gooseberry fruit (*Emblica officinalis*) and its removal from electroplating wastewater, Desalination 277 (2011) 390–398.
[19] N.T. Abdel-Ghani, G.A. El-Chaghaby, Biosorption for metal ions removal from aqueous solutions: A review of recent studies, Int. J. Latest Res. Sci. Technol. 3 (2014) 24–42.
[20] K.C. Sekhar, C.T. Kamala, N.S. Chary, A.R. Sastry, T.N. Rao, M. Viramani, Removal of lead from aqueous solution using an immobilized biomaterial derived from plant biomass, J. Hazard. Mater. 108 (2004) 111–117.
[21] A. Esposito, F. Pagnanelli, A. Lodi, C. Solisio, F. Vegliò, Biosorption of heavy metals by *Sphaerotilus natans*: An equilibrium study at different pH and biomass concentrations, Hydrometallurgy 60 (2001) 129–141.
[22] C.P.J. Isaac, A. Sivakumar, Removal of lead and cadmium ions from water using *Annona squamosa* shell: Kinetic and equilibrium studies, Desalin. Water Treat. 51 (2013) 7700–7709.
[23] A. Zubair, H.N. Bhatti, M.A. Hanif, F. Shafqat, Kinetic and equilibrium modeling for Cr(III) and Cr(VI) removal from aqueous solutions by *Citrus reticulata* waste biomass, Water Air Soil Pollut. 191 (2008) 305–318.
[24] R.M. Gabr, S.H.A. Hassan, A.A.M. Shoreit, Biosorption of lead and nickel by living and non-living cells of *Pseudomonas aeruginosa* ASU 6a, Int. Biodeterior. Biodegrad. 62 (2008) 195–203.
[25] R. Say, A. Denizli, M. Yakup Arıca, Biosorption of cadmium(II), lead(II) and copper(II) with the filamentous fungus *Phanerochaete chrysosporium*, Bioresour. Technol. 76 (2001) 67–70.
[26] S.E. Oh, S.H.A. Hassan, J.H. Joo, Biosorption of heavy metals by lyophilized cells of *Pseudomonas stutzeri*, World J. Microbiol. Biotechnol. 25 (2009) 1771–1778.
[27] S. Özdemir, E. Kılınç, A. Poli, B. Nicolaus, Biosorption of Heavy Metals (Cd^{2+}, $Cu2^{+}$, Co^{2+}, and Mn^{2+}) by thermophilic bacteria, *Geobacillus thermantarcticus* and *Anoxybacillus amylolyticus*: Equilibrium and kinetic studies, Bioremediat. J. 17(2013) 86–96.
[28] O.F. Okeola, E.O. Odebunmi, O.M. Ameen, Comparison of sorption capacity and surface area of activated carbon prepared from *Jatropha curca* fruit pericarp and seed coat, Bull. Chem. Soc. Ethiop. 26 (2002) 171–180.
[29] G. Dönmez, Z. Aksu, Removal of chromium(VI) from saline wastewaters by *Dunaliella* species, Process Biochem. 38 (2002) 751–762.
[30] T. Fan, Y. Liu, B. Feng, G. Zeng, C. Yang, M. Zhou, H. Zhou, et al., Biosorption of cadmium(II), zinc(II) and lead(II) by *Penicillium simplicissimum*: Isotherms, kinetics and thermodynamics, J. Hazard. Mater. 160 (2008) 655–661.
[31] G. Ozdemir, N. Ceyhan, T. Ozturk, F. Akirmak, T. Cosar, Biosorption of chromium(VI), cadmium(II) and copper(II) by *Pantoea* sp. TEM18, Chem. Eng. J. 102 (2004) 249–253.
[32] S. Naik, I. Furtado, Equilibrium and kinetics of adsorption of Mn^{2+} by Haloarchaeon *Halobacterium* sp. GUSF (MTCC3265), Geomicrobiol. J. 31 (2014) 708–715.
[33] S. Lagergren, About the theory of so-called adsorption of soluble substances, K Sven Vetenskapsakad Handl 24 (1898) 1–39.
[34] Y.S. Ho, G. Mckay, The kinetics of sorption of basic dyes from aqueous solution by sphagnum moss peat, Can. J. Chem. Eng. 76 (1998) 822–827.
[35] Y. Qu, H. Li, A. Li, F. Ma, J. Zhou, Identification and characterization of *Leucobacter* sp. N-4 for Ni(II) biosorption by response surface methodology, J. Hazard. Mater. 190 (2011) 869–875.
[36] U.C. Naik, S. Srivastava, I.S. Thakur, Isolation and characterization of *Bacillus cereus* IST105 from electroplating effluent for detoxification of hexavalent chromium, Environ. Sci. Pollut. Res. 19 (2012) 3005–3014.
[37] D.P. Higham, P.J. Sadler, M.D. Scawen, Effect of cadmium on the morphology, membrane integrity and permeability of *Pseudomonas putida*, J. Gen. Microbiol. 132 (1986) 1475–1482.
[38] V.K. Adarsh, M. Mishra, S. Chowdhury, M. Sudarshan, A.R. Thakur, S. Ray Chaudhuri, Studies on metal microbe interaction of three bacterial isolates from east Calcutta wetland, online, J. Biol. Sci. 7 (2007) 80–88.
[39] P. Singh, C. Raghukumar, R.R. Parvatkar, M.B.L. Mascarenhas-Pereira, Heavy metal tolerance in the psychrotolerant *Cryptococcus* sp. isolated from deep-sea sediments of the Central Indian Basin, Yeast 30 (2013) 93–101.
[40] S.K. Kazy, S.F. D'Souza, P. Sar, Uranium and thorium sequestration by a *Pseudomonas* sp.: Mechanism and chemical characterization, J. Hazard. Mater. 163 (2009) 65–72.
[41] M.L. Merroun, J. Raff, A. Rossberg, C. Hennig, T. Reich, S. Selenska-Pobell, Complexation of uranium by cells

and S-layer sheets of *Bacillus sphaericus* JG-A12, Appl. Environ. Microbiol. 71 (2005) 5532–5543.
[42] A. Sari, M. Tuzen, Biosorption of Pb(II) and Cd(II) from aqueous solution using green alga (*Ulva lactuca*) biomass, J. Hazard. Mater. 152 (2008) 302–308.
[43] R. Rajaram, J. Sumitha Banu, K. Mathivanan, Biosorption of Cu(II) ions by indigenous copper-resistant bacteria isolated from polluted coastal environment, Toxicol. Environ. Chem. 95 (2013) 590–604.
[44] K. Finneran, R. Anderson, K. Nevin, D. Lovley, Potential for bioremediation of uranium-contaminated aquifers with microbial U(VI) reduction, Soil Sediment Contam.: Int. J. 11 (2002) 339–357.